Semidilute Solutions of Liquid Crystalline Polymers

Walter Richtering,* Wolfgang Gleim, and Walther Burchard

Institut für Makromolekulare Chemie, Universität Freiburg, Stefan-Meier Strasse 31, D-7800 Freiburg, Germany

Received November 13, 1991; Revised Manuscript Received March 30, 1992

ABSTRACT: Solution properties of two liquid crystalline side-chain polymers of different architecture have been investigated by static and dynamic light scattering. Dilute solutions of these polymers showed common flexible chain behavior, and no indications for a significant chain rigidity were observed. In semidilute solution the concentration dependence of the osmotic modulus revealed stronger repulsion than common linear macromolecules. Furthermore, a chain-length dependence was observed. Both effects can be explained by the thickness of the polymer chain. At high concentrations an excess low-angle scattering and a slow mode of motion were detected, indicating formation of large clusters. The first appearance of these clusters was found at the same concentration for samples of different molar mass. This leads to the suggestion that attractive interactions between mesogenic groups are responsible for cluster formation. Further information on the structure of the clusters was obtained by studying fractal dimension and depolarized scattered light.

1. Introduction

Semidilute solutions have been the object of intense research for the last few years.[1-5] In semidilute solutions a strong interpenetration of the macromolecular coils is assumed, which leads to the formation of a homogenous entanglement network. Due to entanglements the influence of the individual chain on the solution's properties is negligible and molecular weight independence is expected, if the concentration exceeds the overlap concentration c^*. Application of scaling and renormalization group theory has led to comprehensive description of semidilute solutions. One example is the concentration dependence of the osmotic modulus $(1/RT)(\partial\pi/\partial c)$ as measured by static light scattering. Polymers of different architectures have been investigated, and good agreement has been found for flexible linear chains. Different architectures show characteristic deviations.

There are, however, some experimental findings which are not in agreement with the existence of a homogenous entanglement network. (i) In static light scattering an increase of intensity at small scattering angles is observed,[6,7] causing a turnover of the osmotic modulus. (ii) In dynamic light scattering a slow mode of motion appears in the time correlation function. Due to the fact that in many cases both observations appear simultaneously, it was suggested that big particles (or in different terms, long-range heterogenities) are formed which cause a low-angle excess scattering and a slow diffusion.[8,9] Many polymers of different structure and architecture have been studied so far, and cluster formation seems to be a universal behavior of semidilute solutions at least in good and marginal solvents. There may be some distinctions in θ-solvents.[10,11] Although experimental observation of these big particles is now widely accepted, the reasons for their formation are not yet totally understood. Topological constraints can be one reason, and as a consequence, the appearance of clusters should be determined by c/c^*. Then a molecular weight dependence should arise because c^* depends on molecular weight. Specific interactions between chain segments can be a second reason for cluster formation, and this process should be describable by a chemical reaction constant.

In this contribution we present results obtained by light scattering from semidilute solutions of thermotropic liquid crystalline (LC) side-chain polymers. Liquid crystalline polymers have been known for many years, and their bulk properties are under particular investigation.[12,13] Only a few studies deal with the solution properties.[14-16] In a recent paper we reported a study on dilute solution behavior of LC side-chain polymers, especially investigating the influence of the solvent.[17] Common flexible chain behavior was found. This paper concerns the influence of the degree of polymerization on semidilute solutions. Two different systems have been studied (see Figure 1a,b). In the first case the mesogenic group is laterally attached to the polymer backbone via a long flexible spacer. In the second case the mesogen is directly fixed to the backbone. For obvious reasons the former system will be called side-on, the latter end-on.

2. Experimental Section

Synthesis of the monomers was performed as described in the literature.[18,19] Radical polymerization was carried out in benzene at 60 °C with AIBN as initiator. The refractive index increment was measured with a Brice Phoenix differential refractometer at 20 °C. The results are given in Table I.

For the LS experiments an automatic ALV goniometer and an ALV correlator ALV 3000 was used. In semidilute solution time correlation functions were measured in the multi-τ mode using 192 channels, starting with STC = 1 μs, plus 16 fast real-time channels with STC = 60 ns. As light source an argon ion laser (λ_0 = 488 or 496.5 nm) and a krypton ion laser (λ_0 = 647.1 nm) were used. The measurements were performed in the angular range from 20° to 150° in steps of 5° or 10°. When small-angle excess scattering was observed, some measurements were carried out every 2° in the range from 16° to 40°.

Dilute solutions were filtered through Millipore filters (Millex HV 0.45 μm) directly into dustfree cells. Higher concentrated solutions were prepared as follows: A dilute solution was prepared as described above, and LS experiments were performed with this solution. If it was free of dust, some solvent was evaporated from the cell by placing the cell with the lid removed inside a laminar flowbox. The concentration was determined by weighing the cell. This procedure could not be performed in a moisture-free environment, and the residual water content could have changed upon concentrating the solution. Therefore this preparation procedure was checked by preparing solutions which still could be filtered. Results of LS measurements obtained from samples prepared by both techniques were in excellent agreement with each other, indicating that possible changes of the water content did not affect the LS results.

A high-quality Glan-Thomson prism (Bernhard Halle Nachfolger, Berlin) was used to measure the depolarized component of the scattered light. The alignment was checked by measuring the ratio of depolarization of toluene and chloroform. At high concentrations, fluorescence was observed and therefore an interference filter was used in front of the photomultiplier.

0024-9297/92/2225-3795$03.00/0

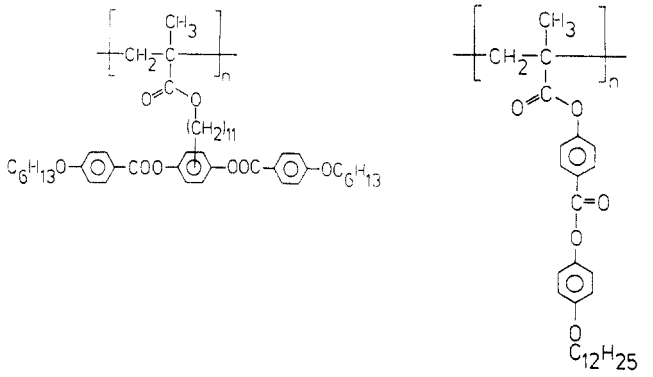

Figure 1. (a, left) Chemical formula of the repeating unit of the side-on polymers. (b, right) Chemical formula of the repeating unit of the end-on polymers.

3. Results and Discussion

3.1. Dilute Solutions. Static light scattering from dilute polymer solutions is described by[20]

$$\frac{Kc}{R(\theta)} = \frac{1}{M_w}(1 + \langle s^2\rangle_z q^2/3) + 2A_2c + 3A_3c^2 + \dots \quad (1)$$

where K is an optical contrast factor that includes the refractive index increment dn/dc, $R(\theta) = i(\theta)r^2/I_0$ is the Rayleigh ratio, with $i(\theta)$ and I_0 the scattering intensity at scattering angle θ and the primary beam intensity, respectively, r is the distance of the detector from the scattering center, c is concentration, M_w is the weight average of the molar mass, $\langle s^2\rangle_z$ is the z-average mean square radius of gyration, q is the magnitude of the scattering vector $\mathbf{q} = (4\pi/\lambda)\sin(\theta/2)$ (with λ wavelength of the light in the solution), and A_2 and A_3 denote the second and third osmotic virial coefficients.

The initial slope of the time correlation function of dynamic light scattering was determined by a cumulant fit. From the first cumulant Γ, the mutual diffusion coefficient was determined from extrapolation of $D_{app} = \Gamma/q^2$ to zero angle.[21] In dilute solution the concentration dependence can be described by the linear equation

$$D_c = D_z^0(1 + k_D c) \quad (2)$$

By use of the Stokes–Einstein relation $D_z = [k_B T/(6\pi\eta_0 R_h)]_z$, an equivalent hydrodynamic radius R_h is calculated from the diffusion coefficient at infinite dilution D_z^0.

Additional information on the structure can be obtained from the ρ-parameter[22] $\rho = \langle s^2\rangle_z^{0.5}\langle 1/R_h\rangle_z$ and from the equivalent thermodynamic hard-sphere radius R_{eq}, which is calculated with the aid of the equation for hard spheres[23]

$$A_2 = 4N_A V_m/M^2 \quad (3)$$

where N_A is Avogadro's constant and $V_m = (4\pi/3)R_{eq}^3$ is the hard-sphere volume.

When this study was starting, it was not clear whether there was an influence of the solvent on the solution structure. It was reported in the literature[14] that chloroform does not lead to an aggregation of LC polymers, and therefore, the characterization of the side-on samples was performed in $CHCl_3$. Comparing LS results from similar LC polymers in different solvents, we found no influence of the solvent on the solution structure[17] and used tetrahydrofuran as solvent for the end-on samples because of a higher dn/dc value and also for environmental reasons.

A static and a dynamic Zimm plot is shown in Figure 2a,b, and the results from extrapolation to zero angle and

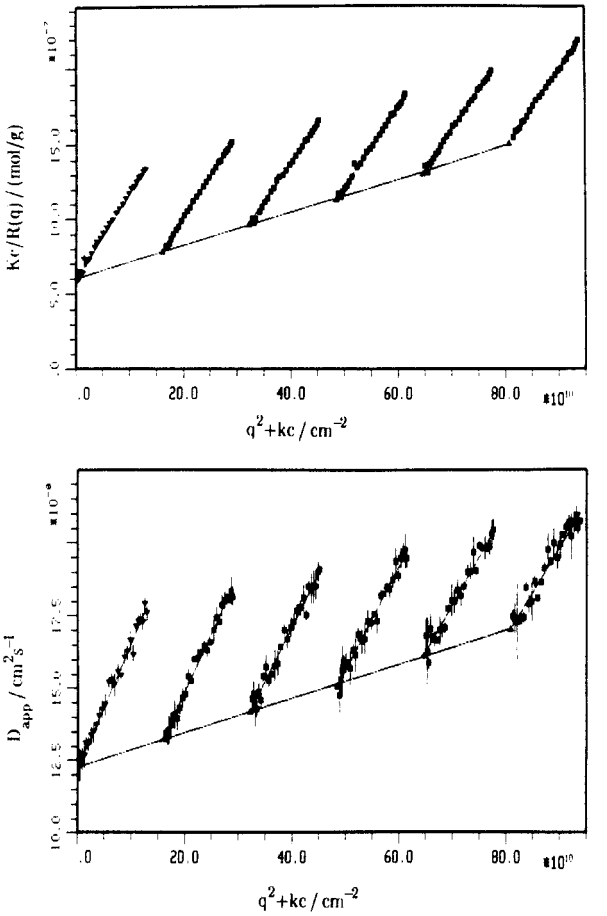

Figure 2. Static (a, top) and dynamic (b, bottom) Zimm plots of so-1 in $CHCl_3$.

Table I
Refractive Index Increments of Side-On Polymers in $CHCl_3$ and End-On Polymers in THF

side-on		end-on	
λ_0, nm	dn/dc, cm³/g	λ_0, nm	dn/dc, cm³/g
488	0.113	488	0.149
514	0.110	496.5	0.148
647.1	0.101	647.1	0.138

zero concentration are summarized in Table II. Common behavior of flexible macromolecules was observed in both cases; no indications for a significant chain rigidity were found. The ρ-parameter of monodisperse, flexible coils was calculated to be in the range 1.25–1.56 depending on the quality of the solvent.[24] For polymers with a polydispersity of $M_w/M_n = 2$ the ρ-parameter increases by 15%, yielding $\rho = 1.8$ in good solvents.[25] Using the theoretical calculations of Akcasu and Benmouna, $\rho = 2.1$ is determined.[26] The experimentally observed values fall in the range 1.7–2.1 and thus obey behavior typical of polydisperse linear chains.

3.2. Semidilute Solutions. A characteristic Zimm plot at high concentration is shown in Figure 3. With the side-on system, a small-angle excess scattering is observed at concentrations above 120 g/L. Obviously the solution is no longer homogenous, but long-range heterogenities are observed. Therefore the discussion of results will be divided into two parts: (i) measurements at large scattering angles, which probe properties of the entanglement network, and (ii) measurements at small angles, which probe properties of the clusters. Measurements at large scattering angle are described at first.

(a) Osmotic Modulus. From light scattering at zero scattering angle one obtains the inverse osmotic com-

Table II
Results from Static and Dynamic Light Scattering of Side-On Polymers in $CHCl_3$ and End-On Polymers in THF

	M_w, g/mol	DP_w	A_2, mol·cm³ g⁻²	R_{eq}, nm	$\langle s^2\rangle_z^{0.5}$, nm	$10^7 D_z^0$, cm²/s	k_D, cm³/g	R_h, nm	ρ
so-1	1.89×10^6	2500	8.09×10^{-5}	30.5	55	1.22	78	30.2	1.82
so-2	1.68×10^5	222	2.34×10^{-4}	8.7		4.98	12	7.4	
so-3	5.47×10^4	72	2.49×10^{-4}	4.2		6.14	4	6.0	
eo-1	1.25×10^6	2680	1.34×10^{-4}	27.5	55	1.39	120	31.8	1.72
eo-2	2.03×10^5	436	2.98×10^{-4}	10.7	25	3.71	33	11.9	2.09
eo-3	8.00×10^4	172	3.2×10^{-4}	5.9		6.21	11	7.1	

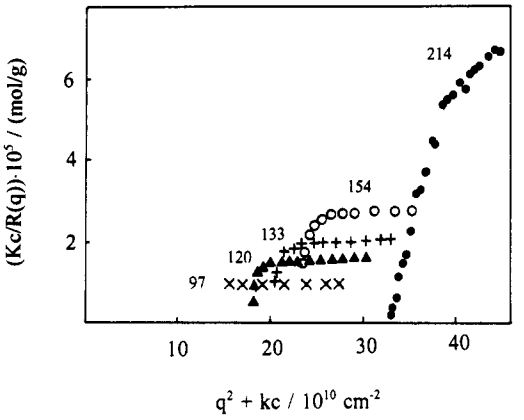

Figure 3. Zimm plot of so-1 in $CHCl_3$ at high concentrations. The numbers denote the concentration in grams per liter.

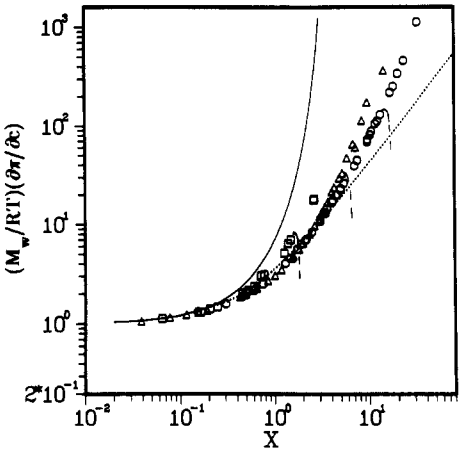

Figure 4. Plot of the reduced osmotic modulus of the side-on samples in $CHCl_3$ vs the parameter $X = A_2M_wc$: so-1 (○), so-2 (△), so-3 (□), hard spheres (—), flexible chains (···).

pressibility (osmotic modulus)[23]

$$\frac{Kc}{R_{\theta=0}} = \frac{1}{M_{app}} = \frac{1}{RT}\frac{\partial \pi}{\partial c} \tag{4}$$

with M_{app} an apparent molar mass and π the osmotic pressure. At high scattering angles no angular dependence is observed in static light scattering, and extrapolation to zero angle delivers the osmotic modulus of the entanglement network. Theory shows that the normalized osmotic modulus $(M_w/RT)(\partial\pi/\partial c)$ is a function of the dimensionless parameter $X = A_2M_wc$.[2-4] This parameter is proportional to c/c^*. Hence the parameter X provides a thermodynamic definition of the overlap concentration. It is known that for linear macromolecules of different molar mass a common curve is obtained in a plot of the osmotic modulus vs the parameter X.[4] Polymers of different architectures show characteristic deviations; star-like or statistically branched polymers exhibit stronger repulsion than linear chains, whereas stiff macromolecules show less.[5]

In Figures 4 and 5, the reduced osmotic moduli are plotted vs the parameter X for both systems. For

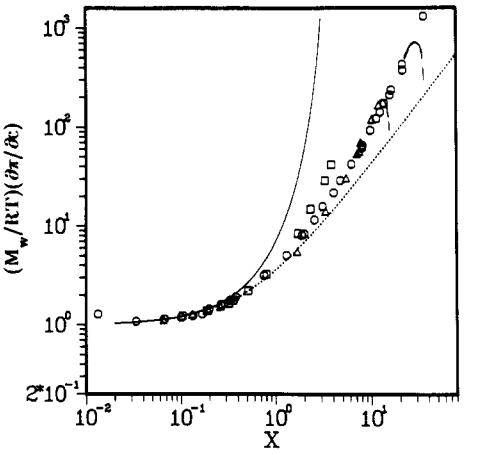

Figure 5. Plot of the reduced osmotic modulus of the end-on samples in THF vs the parameter $X = A_2M_wc$: eo-1 (○), eo-2 (△), eo-3 (□), hard spheres (—), flexible chains (···).

comparison, theoretical curves of hard spheres (Carnahan–Starling formula[27]) and flexible chains (renormalization group theory RG[28]) are also shown. In both systems, deviations from common behavior are observed. (i) Even the samples with the highest molar mass (so-1, eo-1) show stronger repulsion, as was found for polystyrene. (ii) A strong influence of the degree of polymerization is observed.

In the case of the liquid crystalline side-chain polymers, the deviations can be explained in terms of the thickness of the polymer chain. Due to the bulky side group, the excluded volume effect of one chain segment is larger than in common linear macromolecules causing a stronger monomer–monomer self-interaction. In RG theory a cutoff parameter takes care of this type of polymer self-interaction, which is effective at short chain length.[3] Obviously in liquid crystalline polymers longer chains are necessary in order to obtain typical macromolecular behavior, which is defined by a vanishing influence of the chain microstructure. However, even the longest chains show stronger repulsion (slopes of 1.84 for so-1 and 1.9 for eo-1) than polystyrene (slope 1.4).[4] Comparison between the two systems reveals that the manner in which the mesogenic group is attached to the polymer backbone has no significant influence on the osmotic modulus.

At small scattering angles the intensity increases strongly and causes a turnover of the osmotic modulus. This behavior is shown by the dashed curves in Figures 4 and 5. A more quantitative extrapolation to zero angle was not possible due to the very pronounced angular dependence. This steep slope indicates that very big clusters are formed, the properties of which will be discussed later; first dynamic properties of the entanglement network are described.

(b) Cooperative Diffusion. In semidilute solution dynamic light scattering probes the cooperative diffusion of the entanglement network. The mutual diffusion at finite concentration is determined by both hydrodynamic and thermodynamic forces. Irreversible thermodynamics

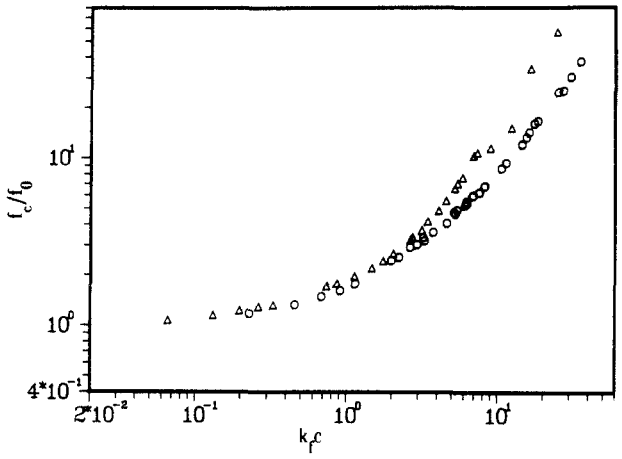

Figure 6. Plot of the reduced friction coefficient of the side-on polymers in $CHCl_3$ vs k_fc: so-1 (○), so-2 (△).

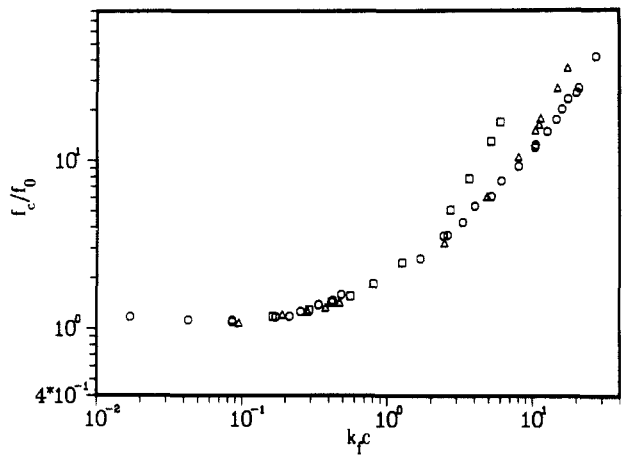

Figure 7. Plot of the reduced friction coefficient of the end-on polymers in THF vs k_fc: eo-1 (○), eo-2 (△), eo-3 (□).

shows that the concentration dependence is given by[23]

$$D_c = (k_B T/f_c)[(M_w/RT)(\partial\pi/\partial c)] \quad (5)$$

where k_B is Boltzmann's constant and f_c is the strongly concentration-dependent friction coefficient. From scaling theory an asymptotic power law was calculated for the concentration dependence of the cooperative diffusion coefficient $D_c \propto c^{0.75}$.[1] The time correlation function of concentrated solutions of the side-on samples consisted not only of the cooperative diffusion of the entanglement network but also of a slow mode. Therefore the time correlation function was analyzed by inverse Laplace transformation using Provencher's CONTIN program.[29] The results for the cooperative diffusion coefficient are summarized in Table II. The term inside the brackets in eq 5 is the reduced osmotic modulus; thus by combining static and dynamic light scattering the friction coefficient can be determined.

$$f_c = (k_B T/D_c)M_w(Kc/R_{\theta=0}) \quad (6)$$

In dilute solution the concentration dependence of the friction coefficient can often be approximated by the linear equation

$$f_c = f_0(1 + k_f c) \quad (7)$$

The concentration dependences of D_c and f_c are related to each other[23]

$$k_D = 2A_2M_w - k_f - \bar{v}_2 \quad (8)$$

with $\bar{v}_2$ the partial specific volume of the polymer.

From the concentration dependences of π, D_c, and f_c it can be seen that various definitions of c^* are possible:

$$c^* = 1/A_2M_w \quad \text{thermodynamic}$$

$$c^* = 1/k_f \quad \text{hydrodynamic}$$

$$c^* = 1/k_D \quad \text{diffusive}$$

It was already mentioned that $X = A_2M_wc$ is a suitable scaling parameter for the osmotic modulus. In contrast, from results with linear polystyrene, X is known not to be a good scaling parameter for dynamic properties.[30] Better scaling is instead observed if k_fc is used, but a certain molecular weight dependence remains still noticeable. In Figures 6 and 7, the reduced friction coefficient for the liquid crystalline polymers is plotted vs k_fc, and again an influence of molar mass is observed. The mutual diffusion coefficient depends on thermodynamic *and* hydrodynamic

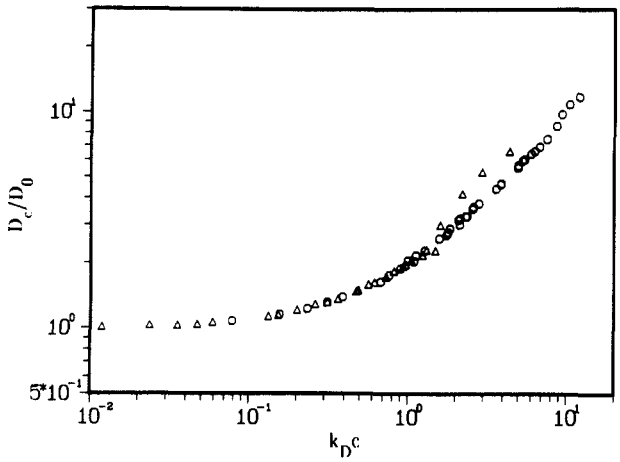

Figure 8. Plot of the reduced diffusion coefficient of the side-on polymers in $CHCl_3$ vs k_Dc: so-1 (○), so-2 (△).

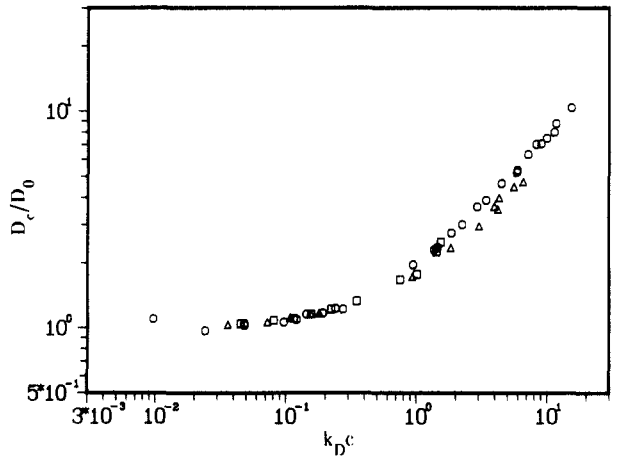

Figure 9. Plot of the reduced diffusion coefficient of the end-on polymers in THF vs k_Dc: eo-1 (○), eo-2 (△), eo-3 (□).

forces, and therefore, both X and k_fc are not expected to be good scaling parameters for D_c. Indeed, plots of D_c/D_0 vs X or k_fc obey nearly the same nonscaling behavior. The smallest influence of chain length is observed if k_Dc is used (see Figures 8 and 9). This is a reasonable observation because k_D contains both influences.

(c) Cluster Formation. The existence of large clusters is obvious from the simultaneous appearance of small-angle excess scattering (Figure 3) and a slow mode in the time correlation function (TCF) (see Figure 10). In the case of the side-on polymers, some properties of the long-range heterogeneities could be studied in detail. Exper-

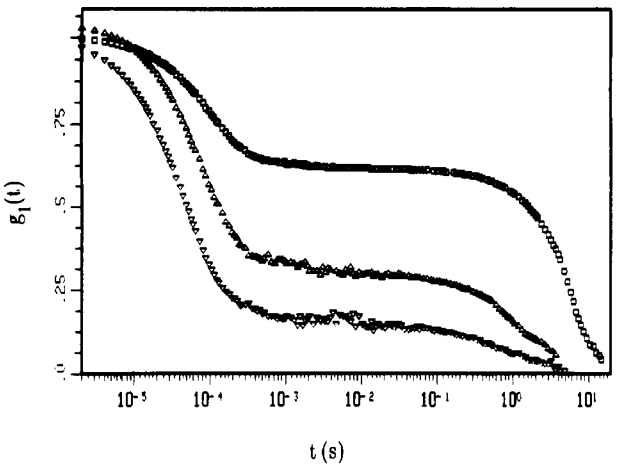

Figure 10. TCF of so-1 at $c = 133$ g/L and $\theta = 25°, 30°$, and 40°, from top to bottom.

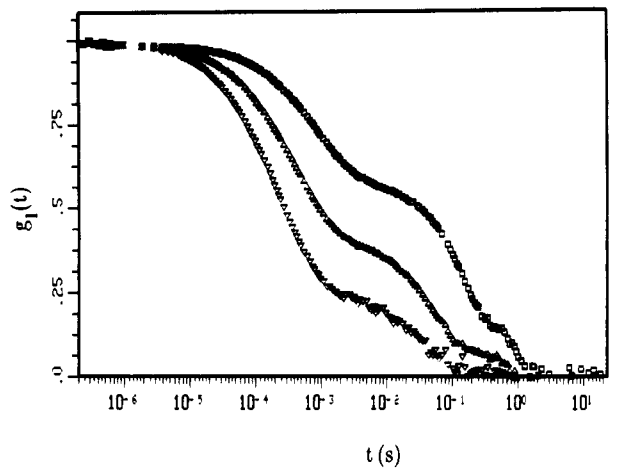

Figure 11. TCF of so-3 at $c = 138$ g/L and $\theta = 20°, 30°$, and 40°, from top to bottom.

Table III
CONTIN Analysis Results of the Time Correlation Function of the Side-On Polymers in $CHCl_3$

so-1		so-2		so-3	
c, g/L	$10^6 D_{coop}$, cm^2/s	c, g/L	$10^6 D_{coop}$, cm^2/s	c, g/L	$10^7 D_{coop}$, cm^2/s
110	1.06	134	1.50	138	5.4
120	1.20	185	2.10	148	5.5
133	1.33	246	2.65	196	4.3
153	1.45	370	3.3		
213	3.6				

imental problems arose with the end-on samples because cluster formation was observed only at concentrations above 200 g/L. Some examples of time correlation functions are shown in Figures 10–12. A few points are worth noting.

(i) A strong angular dependence of the plateau value is observed as well as of the long relaxation time, again indicating that the clusters have to be very large. Here the same problem arises as in static light scattering: Extrapolation of the slow diffusion coefficient to zero angle is not possible. Therefore a quantitative analysis of the time correlation function is limited to the cooperative diffusion (see Table III), and the slow mode can be discussed qualitatively only. Figures 10 and 11 show the time correlation functions of so-1 and so-3 at nearly the same concentration, and the strong influence of molar mass on the slow mode is obvious. The concentration dependence of the slow mode at a finite scattering angle can be seen in Figure 12. It is much stronger than the concentration dependence predicted for a reptation process.

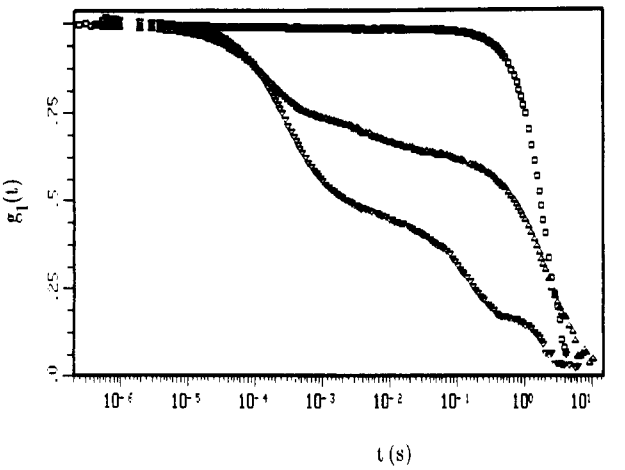

Figure 12. TCF of so-2 at $\theta = 20°$ and $c = 370, 250, 130$ g/L, from top to bottom.

(ii) The time correlation function consists of at least three mean relaxation times (see Figures 11 and 12). The angular dependence of the middle one cannot be described satisfactorily due to the strong angular dependence of the slow mode. However, the existence of this third process is unambiguous, and a possible explanation of this relaxation process could be a decomposition of the cluster as a whole.

(iii) *Most important*, however, is the result that the concentration where clusters are observed for the first time is the same for *all* three side-on samples ($c_{cluster} \approx 120$ g/L). This means a cluster formation which is independent of chain length and independent of the overlap concentration. The dependence of structure growth on concentration supports the model that specific interactions are responsible for the formation of clusters. In such a model the segment concentration at the onset of the turnover for $\partial\pi/\partial c$ is necessarily independent of the degree of polymerization of the original chains. In the liquid crystalline polymer systems, mesogenic groups might be responsible for such clustering.

Two further properties of the clusters have been studied in order to obtain information on the cluster's structure, i.e., the fractal dimension of the clusters and the depolarization of light.

Fractal Dimension. If a particle's density depends on its mass, the scattering intensity is given by[31]

$$I(q) \propto q^{-d} \tag{9}$$

d is the fractal dimension which is defined by the relationship between mass and radius of the particle $M \propto R^d$. In Figure 13, a double-logarithmic plot of I vs q is shown. Slopes close to −3 were found at different concentrations, indicating that the clusters are homogeneous and isotropic. However, eq 9 can only be applied for particles with a correlation length $\xi > 1/q$, and therefore, only particles of a certain size can be investigated in the limited q-range of light scattering.

Depolarization. In most light scattering experiments, polarized light is used and both scattered and irradiated light have the same plane of polarization if the scattering centers are isotropic. If, however, the polarizability is anisotropic, the scattered light consists of two parts: one with the same plane of polarization ("polarized"); the second with a plane of polarization perpendicular to that of the primary beam ("depolarized"). A ratio of depo-

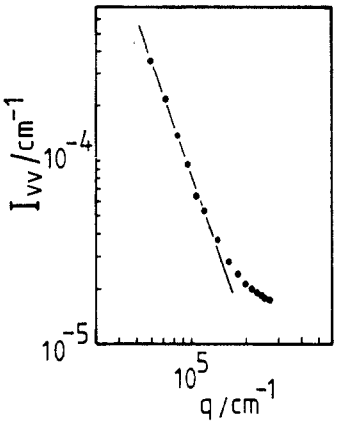

Figure 13. Double-logarithmic plot of scattering intensity vs scattering vector for so-2 at c = 370 g/L.

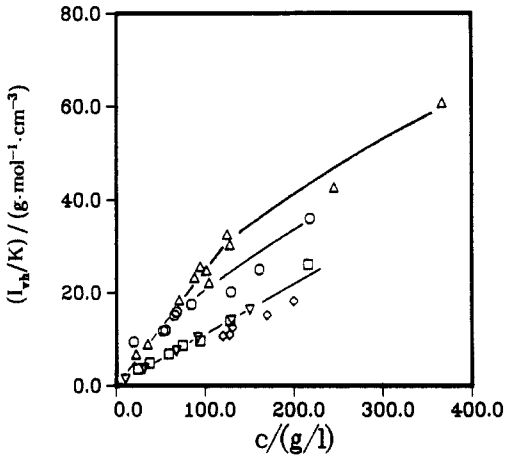

Figure 14. Concentration dependence of depolarized scattering intensity: so-1 (○), so-2 (△), eo-1 (□), eo-2 (◇), eo-3 (▽).

larization can be defined

$$\rho_v = I_{vh}/I_{vv} \tag{10}$$

Here the first index denotes the plane of polarization of the laser beam; the second denotes that of the scattered light. Horn and Benoit[32,33] calculated the depolarized scattering intensity for a model of Gaussian chains built up by anisotropic segments. They obtained for scattering from dilute solutions

$$I_{vh} = I_0 K c \frac{3}{5}\frac{M}{N}\delta^2 \tag{11}$$

with K the optical contrast factor and N the number of statistically independent segments. δ describes the anistropy of polarizability.

$$\delta = (\alpha - \beta)/(\alpha + 2\beta) \tag{12}$$

α and β are the polarizabilities parallel and perpendicular to the axis of a cylindrical chain segment, respectively. According to eq 11, the depolarized intensity from Gaussian chains only depends on concentration and δ, but not on molecular weight. In Figure 14, a plot of depolarized intensity vs concentration is shown. Measurements were performed at two wavelengths (496.5 and 647.1 nm), and the intensity was normalized by the contrast factor K. At concentrations below the onset of cluster formation, linear behavior with respect of c is observed, with no correlations between mesogenic groups. In the side-on system, a slight angular dependence (small increase at low angles) is observed at concentrations above $c_{cluster}$, but not as pronounced as the increase of the polarized component. In Figure 14, measurements at large angles are plotted and deviations from the linear dependence to smaller

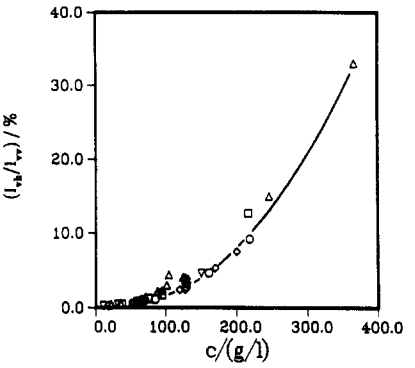

Figure 15. Concentration dependence of the ratio of depolarization: so-1 (○), so-2 (△), eo-1 (□), eo-2 (◇), eo-3 (▽).

values are observed, but no large oriented regions seem to exist. However, it is possible that correlations between mesogenic groups on a short-length scale might be sufficient to cause formation of big clusters and stabilize them. The next important aspect of anisotropy can be seen from the ratio of depolarization in Figure 15. Again, at $c > c_{cluster}$, measurements at large scattering angles are plotted. At small concentrations the ratio is less than 1%, i.e., the Cabannes factor[34] of these liquid crystalline polymers is nearly 1 and thus lies in the same range as common polymers. If, however, the osmotic modulus of the entanglement network at $c > c_{cluster}$ is to be determined, the depolarized part has to be subtracted from the total scattering intensity. The strong increase of the depolarization ratio is not due to an increase of I_{vh} but is a consequence of the decrease of I_{vv} due to repulsive osmotic forces.

From measurements of ordinary and extraordinary refractive indexes in the liquid crystalline phase, Hessel et al.[18] and Finkelmann et al.[35] determined the anisotropy of polarizability of similar LC side-chain polymers applying Haller plots.[36] They obtained

$$\delta = 0.13 \quad \text{(side-on)}$$

$$\delta = 0.12 \quad \text{(end-on)}$$

If these values are used in eq 11, the mass of a statistical chain segment can be estimated. Approximately five to seven monomeric units were found to form one segment, showing that these liquid crystalline side-chain polymers are rather flexible.

4. Conclusions

In dilute solution liquid crystalline polymers behave like common flexible chain molecules. Even in the case of the end-on polymers where the mesogenic group is directly attached to the polymer backbone, no indications for a significant chain stiffness are observed by light scattering. This is in contrast to the liquid crystalline behavior of the polymer in bulk, where a strong influence of architecture and length of the flexible spacer on the LC-phase behavior was observed.[19]

In semidilute solution deviations from flexible chain behavior occur. The normalized osmotic modulus reveals stronger repulsion and molecular weight dependence. Both observations can be explained by the macromolecule's rather pronounced thickness.

In the side-on system formation of clusters is observed at a certain concentration *independent* of molecular weight. Therefore we suggest that attractive interactions are responsible for cluster formation. The clusters have to be very large because a very steep angular dependence

of static intensity and apparent diffusion coefficient is observed which makes extrapolation to zero angle impossible. The time correlation function includes at least three different relaxation processes; the middle one, however, is not well characterized and the physical origins are not yet clear. The fractal dimension of clusters was found to be close to 3, indicating a homogeneous structure. From depolarized light scattering it can be assumed that there is no long-range liquid crystalline order inside the clusters. However, the effect of depolarization has to be taken into account if the osmotic modulus of the entanglement network is to be determined.

Acknowledgment. This work was supported by the Deutsche Forschungsgemeinschaft within the Sonderforschungsbereich 60. We thank Dr. F. Hessel for preparation of sample so-1 and E. Stibal-Fischer and M. Schweizer for technical assistance. W. R. thanks the Graduiertenkolleg Polymerwissenschaften for a scholarship.

References and Notes

(1) de Gennes, P.-G. *Scaling Concepts in Polymer Physics*; Cornell: Ithaca, NY, 1979.
(2) Doi, M.; Edwards, S. F. *The Theory of Polymer Dynamics*; Clarendon Press: Oxford, UK, 1986.
(3) Freed, K. *Renormalization Group Theory of Macromolecules*; Wiley: New York, 1987.
(4) Wiltzius, P.; Haller, H. R.; Cannell, D. S.; Schaefer, D. W. *Phys. Rev. Lett.* **1983**, *51*, 1183.
(5) Burchard, W. *Makromol. Chem. Macromol. Symp.* **1988**, *18*, 1.
(6) Koberstein, J. T.; Picot, C.; Benoit, H. *Polymer* **1985**, *28*, 673.
(7) Wendt, E.; Springer, J. *Polymer* **1988**, *29*, 1301.
(8) Eisele, M.; Burchard, W. *Macromolecules* **1984**, *17*, 1636.
(9) Huber, K.; Bantle, S.; Burchard, W.; Fetters, L. J. *Macromolecules* **1986**, *19*, 1404.
(10) Brown, W.; Stepanek, P. *Macromolecules* **1988**, *21*, 1791.
(11) Brown, W.; Johnsen, R.; Stepanek, P.; Jakes, J. *Macromolecules* **1988**, *21*, 2859.
(12) Blumstein, A., Ed. *Polymeric Liquid Crystals*; Plenum: New York, 1985.
(13) Mc Ardle, C. D., Ed. *Side Chain Liquid Crystalline Polymers*; Blackie: Glasgow, 1988.
(14) Springer, J.; Weigelt, F. W. *Makromol. Chem.* **1983**, *184*, 1489, 2635.
(15) Duran, R.; Strazielle, C. *Macromolecules* **1987**, *20*, 2853.
(16) Ohm, H. G.; Kirste, R. G.; Oberthür, R. C. *Makromol. Chem.* **1988**, *189*, 1387.
(17) Richtering, W. H.; Schätzle, J.; Adams, J.; Burchard, W. *Colloid Polym. Sci.* **1989**, *267*, 568.
(18) Hessel, F.; Herr, R. P.; Finkelmann, H. *Makromol. Chem.* **1987**, *188*, 1597.
(19) Finkelmann, H.; Rehage, G. *Adv. Polym. Sci.* **1984**, *60/61*, 99.
(20) Huglin, M. B., Ed. *Light Scattering from Polymer Solutions*; Academic Press: London, 1972.
(21) Berne, B. J.; Pecora, R. *Dynamic Light Scattering*; Wiley: New York, 1976.
(22) Burchard, W.; Schmidt, M.; Stockmayer, W. H. *Macromolecules* **1980**, *13*, 1265.
(23) Yamakawa, H. *Modern Theory of Polymer Solutions*; Harper & Row: New York, 1971.
(24) Oono, Y.; Kohmoto, M. *J. Chem. Phys.* **1983**, *78*, 520.
(25) Burchard, W. *Macromolecules* **1978**, *11*, 455.
(26) Akcasu, A. Z.; Benmouna, M. *Macromolecules* **1978**, *11*, 1187.
(27) Carnahan, N. F.; Starling, K. E. *J. Chem. Phys.* **1969**, *51*, 635.
(28) Ohta, T.; Oono, Y. *Phys. Lett. A* **1982**, *89A*, 460.
(29) Provencher, S. W. *Comput. Phys. Commun.* **1982**, *27*, 213, 229.
(30) Wiltzius, P.; Haller, H. R.; Cannell, D. S.; Schaefer, D. W. *Phys. Rev. Lett.* **1984**, *53*, 834.
(31) Schaefer, D. W.; Martin, J. E.; Hurd, A. J.; Keefer, K. D. In *Physics of Finely Divided Matter*; Boccara, N., Daoud, M., Eds.; Springer Verlag: Berlin, 1985.
(32) Horn, P.; Benoit, H. *J. Polym. Sci.* **1953**, *10*, 29.
(33) Horn, P. *Ann. Phys. (Paris)* **1955**, *10*, 386.
(34) Cabannes, J. *J. Phys. Radium* **1920**, *49*, 129.
(35) Finkelmann, H.; Benthack, H.; Rehage, G. *J. Chim. Phys. (Paris)* **1983**, *80*, 163.
(36) Haller, J.; Huggins, H. A.; Lilienthal, H. R.; Mc Guire, T. F. *J. Phys. Chem.* **1973**, *77*, 950.

Registry No. 2-[11-[(2-Methyl-1-oxo-2-propenyl)oxy]-undecyl]-1,4-phenylene 4-(hexyloxy)benzoate (homopolymer), 103467-68-1; 4-(dodecyloxy)phenyl 4-[(2-methyl-1-oxo-2-propenyl)oxy]benzoate (homopolymer), 81897-12-3.